3D Optical Spectroscopic Methods in Astronomy
ASP Conference Series, Vol. 71, 1995
G. Comte, M. Marcelin, eds.

HIFI Survey of Emission-Line Galaxies: recent Results on the Nuclear Superbubble of NGC 3079

S. Veilleux[1]

Kitt Peak National Observatory, NOAO, Tucson, AZ 85726-6732, USA

G. Cecil

Physics & Astronomy Dept., University of North Carolina, CB# 3255, Chapel Hill, NC 27599-3255, USA

Abstract. The Hawaii Imaging Fabry-Perot Interferometer (HIFI) was used to produce a large data cube of the edge-on SBc galaxy NGC 3079 covering Hα + [N II] $\lambda\lambda$6548, 6583. The complete two-dimensional coverage of the Fabry-Perot data allowed us to derive the general flow pattern of the nuclear gas that constitutes the energetic superbubble.

1. Introduction

A violent, spatially resolved outflow from the nuclear region of the edge-on SB(s)c galaxy NGC 3079 has been detected in the visual long-slit spectra of Heckman, Armus, & Miley (1990; HAM) and Filippenko & Sargent (1992; FS). There is strong evidence for an active galactic nucleus (AGN) and intense star formation (e.g., Duric & Seaquist 1988; Irwin & Seaquist 1988; Young, Claussen, & Scoville 1988). The relative importance of AGN and nuclear starburst in powering the outflow is still unclear. One reason for this uncertainty is the kinematic complexity of the outflowing gas and, therefore, the difficulty in determining accurately its kinetic energy. The long-slit spectra of HAM and FS were only partially successful in defining the geometry and kinematics of the outflowing gas due to their restricted spatial coverage. Here we summarize our study with the Hawaii Imaging Fabry-Perot Interferometer (HIFI: Bland & Tully 1989) at the CFHT. We produced complete line-profile grids of Hα and [N II] $\lambda\lambda$6548, 6583 across the full extent of NGC 3079. We used a finesse 60 etalon (with free spectral range 92 Å at Hα) in its 71st and 72nd orders to obtain a velocity resolution of 70 km s^{-1} (Nyquist sampling). The spectral data cube is a stack of 137 velocity planes and was calibrated in our usual way (Bland & Tully [1989]; Veilleux et al. [1994]).

[1]Hubble Fellow

2. Results

A nearly circular shell of line-emitting gas with an apparent diameter of 13″ or 1.1 kpc at the distance of 17.3 Mpc is clearly seen just east of the nucleus. This bubble-like structure was first pointed out by Ford et al. (1986). The lower detection limit of our data shows that the shell is contiguous at faint levels.

Inspection of profiles across the bubble showed that most of them are composed of 3 distinct velocity systems. The distributions of the velocity centroids are shown in Figure 1. These patterns support FS's contention that we are observing an optically thin bubble, with blue and red components arising from the front and back volumes. An ovoidal bubble with the more pointed extremity located at the nucleus was found to best match the observed morphology of the emission-line structure. Good fits to the observed velocity distribution along the bubble mid-axis were found for $n = 2 - 3$, where $V_{\rm outflow} \sim R^n$, and when the bubble axis is tipped toward us by $\sim 3°$. With this flow field the abrupt decrease in velocities near the top of the bubble arises when the rapidly increasing velocity vector swings into the sky plane, rather than from a rapid deceleration of the flow.

3. Discussion: Time scales, Masses, and Energies

The dynamical time scale of the superbubble can be estimated from the deprojected velocity of the entrained material derived from our kinematic model and the linear dimensions of the bubble:

$$t_{\rm dyn} \approx 1 \times 10^6 \; R_{\rm bubble,kpc} \; V^{-1}_{\rm bubble,1000} \quad {\rm yr}, \tag{1}$$

where $V_{\rm bubble,1000}$ and $R_{\rm bubble,kpc}$ are in units of 1000 km s^{-1} and kpc, respectively.

Assuming Case B recombination conditions at 10^4 K and gas density N_e, the ionized mass involved in the outflow of NGC 3079 is of order $10^7 \; N_e^{-1}$ $M_\odot$. An upper limit on the average gas density of 125 cm^{-3} is obtained from the [S II] $\lambda 6731/\lambda 6716$ ratio derived from complementary long-slit data. This mass is similar to those involved in the well-known outflows in the starburst galaxy M82 ($\sim 2 \times 10^5$ $M_\odot$; Bland & Tully 1988; HAM) and the Seyfert galaxy NGC 1068 ($\sim 2 \times 10^5$ $M_\odot$; Cecil, Bland, & Tully 1990). By deprojecting the observed velocities, we derive a bulk kinetic energy summed across the superbubble of 2 $\times$ 10^{56} N_e^{-1} ergs. This energy may be 10 times larger than the kinetic energies involved in the outflows of M82 ($\lesssim 2 \times 10^{53}$ ergs; Bland & Tully 1988; HAM) and NGC 1068 ($\sim 4 \times 10^{53}$ ergs; Cecil, Bland, & Tully 1990).

The rate of mass outflow can be estimated if it has been constant over the dynamical age of the bubble:

$$\frac{dM}{dt} \simeq \frac{M_{\rm bubble}}{t_{\rm dyn}} = 10 \; M_{\rm bubble,7} \; V_{\rm bubble,1000} \; R^{-1}_{\rm bubble,kpc} \; \gtrsim \; 10 \; N_e^{-1} \quad M_\odot \; {\rm yr}^{-1}, \tag{2}$$

where in principle $M_{\rm bubble,7}$ is the sum of the wind and entrained gas in the outflow (which does not include the "disk" component) in units of 10^7 $M_\odot$.

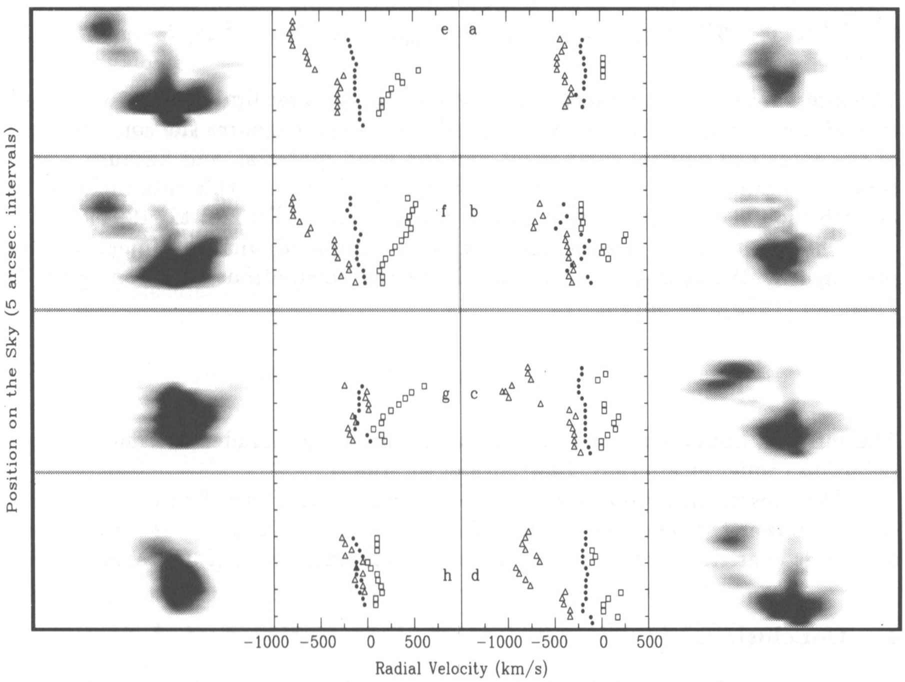

Figure 1. Centroids of the emission-line components in the bubble. Each panel corresponds to a different "long-slit" position across the bubble. The offset between the panels is 2.3″ in declination, with panel *a)* being at the extreme northern edge of the bubble. In each panel, the horizontal axis indicates component radial velocities in km s^{-1} (relative to systemic) and the vertical axis gives positions (right ascensions with arbitrary offsets, 1 unit = 0.″57) along each "long-slit". Three velocity components are observed at most points in the bubble: blueshifted (open triangles) and redshifted (open squares) "bubble" components, and a systemic disk components (small filled circles). Hα line-intensities are shown as greyscales.

However, the value given in equation 2 is a lower limit because it accounts for only the ionized entrained mass. This mass outflow will contribute to the heating and chemical enrichment of the galactic halo of NGC 3079.

Similarly, the input rate of kinetic energy in the outflow of NGC 3079 can be estimated using the same assumptions:

$$\frac{dE_{\rm kin}}{dt} \simeq 3 \times 10^{42} \ \ E_{\rm kin,56} V_{\rm bubble,1000} \, R^{-1}_{\rm bubble,kpc} \ \simeq \ 6 \times 10^{42} \ N_e^{-1} \ \ {\rm erg\ s^{-1}}. \quad (3)$$

The input rate of kinetic energy in equation (3) is a lower limit to the total input rate of energy required to inflate the bubble because it ignores the contributions of the entrained neutral component and the wind material, and because a conservatively small reddening correction was used. Nor does this rate include the contribution of the outflow west of the nucleus (cf. Veilleux et al. 1994).

The input rate of kinetic energy can be compared with the injection rate *predicted* by the starburst scenario. Using the calculations of Elson, Fall, & Freeman (1989), we obtain

$$\frac{dE_*}{dt} = 7 \times 10^{42} \ f_{\rm nuc} \ L_{\rm ir,11} \ \ {\rm erg\ s^{-1}} \ \approx \ 3 \times 10^{41} \ \ {\rm erg\ s^{-1}}. \quad (4)$$

The infrared luminosity used in this calculation only includes the nuclear contribution (Soifer et al. 1987; Lawrence et al. 1985).

The present injection rate of the nuclear starburst therefore appears sufficient to power the observed outflow if $N_e \gtrsim 20$ cm^{-3}. This lower limit on the density is consistent with our long-slit measurements of the [S II] ratio.

4. Conclusions

The violent outflow in NGC 3079 involves an ovoidal bubble of mass $\sim 10^7$ M$_\odot$ N_e^{-1} and kinetic energy $\sim 2 \times 10^{56}$ N_e^{-1} ergs with $N_e < 125$ cm^{-3}. This kinetic energy may be ten times larger than in the outflows in NGC 1068 and M82. Energy arguments suggest that the starburst is powerful enough to drive the outflow. See Veilleux et al. (1994) for a more detailed analysis of these results.

Acknowledgments. We are grateful for support of this research by NSF grants to the Universities of Hawaii and North Carolina. S.V. gratefully acknowledges the financial support of the Natural Sciences and Engineering Research Council of Canada, and NASA through grant number HF-1039.01-92A awarded by the Space Telescope Science Institute which is operated by the AURA, Inc. for NASA under contract No. NAS5–26555.

Discussion

Hippelein: I didn't see the velocity components closing at the upper end of the bubble. Is this because the bubble is not closed?

Veilleux: Yes, indeed. Although there is a clear tendency for the velocity field to converge towards systemic velocity at the top of the bubble, it doesn't quite reach that velocity. This is another indication that the superbubble of NGC 3079 is partially ruptured.

Maillard: Do you see similar bubbles of gas in other starburst galaxies?

Veilleux: Yes, we do. The best example is the famous starburst M 82. The filamentary structure along the poles of this galaxy represents a bipolar outflow over the surfaces of two elongated bubbles (Bland & Tully 1988, Nature, 334, 43). Further evidence for windblown bubbles is also seen in a few other luminous infrared galaxies.

Rocca-Volmerange: You have evidence of ionized gas in your data of NGC 3079. Are you sure that you have evidence of star formation?

Veilleux: The evidence for star formation in NGC 3079 comes from many sources. NGC 3079 has an infrared luminosity similar to that of M 82. Ground-based 10-μm observations suggest that an important fraction of this infrared emission originates in the nucleus. CO measurements indicate the presence of a massive molecular disk centered on the nucleus and coplanar with the galactic disk. Finally, NGC 3079 harbors one of the most luminous H_2O masers known.

References

Bland, J., & Tully, R. B. 1988, Nature, **334**, 43

Bland, J., & Tully, R. B. 1989, AJ, **98**, 723

Cecil, G., Bland, J., & Tully, R. B. 1990, ApJ, **329**, 38

Duric, N. & Seaquist, E. R. 1988, ApJ, **326**, 574

Elson, R. A. W., Fall, S. M., & Freeman, K. C. 1989, ApJ, **336**, 734

Filippenko, A. V., & Sargent, W. L. W. 1992, AJ, **103**, 28(FS)

Ford, H. C., et al. 1986, ApJ, **311**, 7

Heckman, T. M., Armus, L., & Miley, G. K. 1990, ApJS, **74**, 833(HAM)

Irwin, J. A., & Seaquist, E. R. 1988, ApJ, **335**, 658

Veilleux, S., et al. 1994, ApJ, Sept 20th issue

Young, J. S., Claussen, M. J., & Scoville, N. Z. 1988, ApJ, **324**, 115